Hierarchical Nanostructures

DOI: 10.1002/ange.200501960

Bulk Preparation of Si–SiO$_x$ Hierarchical Structures: High-Density Radially Oriented Amorphous Silica Nanowires on a Single-Crystal Silicon Nanocore**

Hui Wang, Xiaohong Zhang, Xiangmin Meng, Shaomin Zhou, Shikang Wu, Wensheng Shi, and Shuittong Lee**

Assembling functional photoelectric nanodevices is of current interest in nanoscience and nanotechnology due to their potential applications in microelectronics and information science.[1] Generally, fabrication routes to a functional nanodevice can be classified into two types: the "top-down" approach and the "bottom-up" approach. The latter refers to assembly or scale up of nanoscale building blocks into functional devices, in which the dimensions of the functional domain can be controlled through the size of the building blocks. Various methods, such as self-assembly and Langmuir–Blodgett (LB) techniques, have been used for fabrication[2] with various degree of success, however, the small size of the nanoscale building blocks makes the fabrication process always costly and complex. Hierarchical nanostructures that have both the properties of nanoscale materials and ease of manipulation may facilitate assembly processes and provide an attractive alternative for bottom-up fabrication. They can be prepared directly by growing nanoscale structures of materials with different dimensions (nanoscale to microscale).[3] In addition, the core and branches of a hierarchical structure can be composed of different chemical elements, making them suitable for assembly into a nanodevice with multiple functions. A few homogeneous and heterogeneous hierarchically structured materials[3] have been fabricated. It is envisaged that these large hierarchical nanostructures could find applications in a variety of fields such as optoelectronics, sensors, and field emission.

Silicon and its oxides have long been of great interest for applications in microelectronic devices, and silicon-on-insulator (SOI) devices are playing an important role in the modern semiconductor industry. Recently, an SiO$_x$–Si hierarchical nanostructure described as "silicon nanowires standing on silica microwires" was fabricated.[4] However, oriented hierarchical nanostructures which are more amenable for device fabrication have yet to be reported. Herein, we report the synthesis of a highly ordered Si–SiO$_x$ columnlike hierarchical nanostructure which consists of high-density, radially oriented amorphous silica nanowires standing on a single-crystal Si nanocore. Unlike the previous hierarchical nanostructures, which were assumed to form by the two-step growth mechanism,[3] the growth of the present Si–SiO$_x$ hierarchical nanostructure appears to occur by two concurrent processes: the vapor–liquid–solid (VLS) mechanism and the oxide-assisted growth (OAG) process. Interestingly, this novel structure emits UV light at 378 nm on excitation by a femtosecond laser at 300 nm.

Si/SiO$_x$ strands were synthesized in a high-temperature tube furnace with tin as catalyst. The general morphology of the deposition product is shown in Figure 1 a–c, which reveals that large-scale wirelike microsized structures are aligned on the substrate, and that the microstructures are long, straight, and smooth strands. The products have diameters of hundreds of nanometers to several micrometers and lengths up to several millimeters (with an aspect ratio exceeding 1.6×10^3). The cross-sectional SEM images (Figure 2 a and b) show that the strands have a columnlike, radially aligned hierarchical structure. Energy dispersive X-ray (EDX) spectroscopy (Figure 2 c and d) confirms the stoichiometric elemental composition of silicon for the core and SiO$_x$ ($x = 1.5$–2) for the branches of the strand. The SEM images further reveal that the strands have two different tip morphologies: one has a corn-shaped taper (Figure 1 d) and the other a spherical particle at the tip (Figure 1 c; EDX confirms the tip is made of Sn, as will be discussed below). It can also be observed that

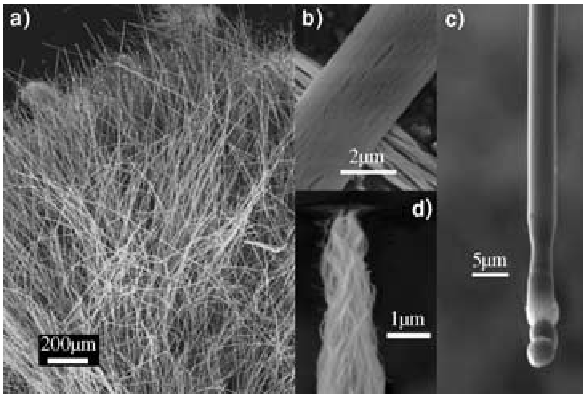

Figure 1. SEM images of as-synthesized Si–SiO$_x$ hierarchical nanostructure.

---

[*] H. Wang, Prof. X.-H. Zhang, Prof. X.-M. Meng, Dr. S.-M. Zhou, Prof. S.-K. Wu, Prof. W.-S. Shi
Nano-organic Photoelectronic Laboratory
Technical Institute of Physics and Chemistry
Chinese Academy of Sciences
Beijing 100101 (China)
Fax: (+86) 10-6487-9375
E-mail: xhzhang@mail.ipc.ac.cn
Prof. S.-T. Lee
Center of Super-Diamond and Advanced Films (COSDAF) and
Department of Physics and Materials Science
City University of Hong Kong
Hong Kong SAR (China)
Fax: (+852) 2784-4696
E-mail: apannale@cityu.edu.hk
H. Wang
Graduate School of Chinese Academy of Sciences
Beijing, 100101 (China)

[**] We thank the Chinese Academy of Sciences and the CAS-Croucher Funding Scheme for Joint Laboratories of the Croucher Foundation for financial support. The work in Hong Kong was supported by the Research Grants Council of Hong Kong SAR, China via a central allocation project (No. CityU 3/04C).

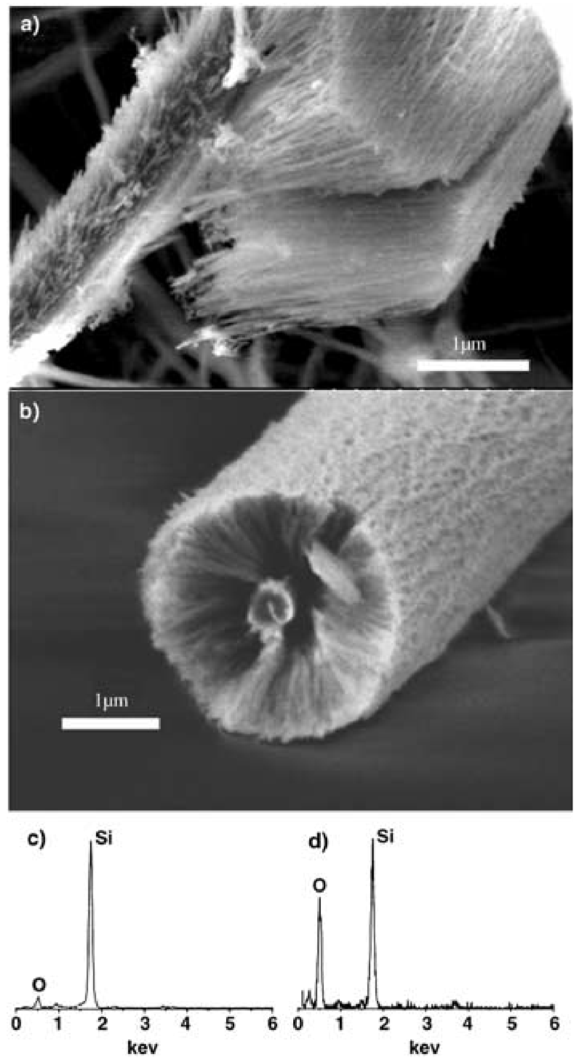

Figure 2. Cross-sectional SEM image of the Si–SiO$_x$ hierarchical structure or strand (a and b) and the corresponding EDX spectra of the core (c) and shell (d) of the strand.

the SiO$_x$ on the strand has fleecy surfaces (Figure 1 d) and grows towards the tapered end where the strand diameter is less than 1 µm. When the diameter is more than 2 µm, the strand looks like a compact whisker or column, and the SiO$_x$ nanowires stand vertically on the strand core (whiskerlike or columnlike; see Figures 1 and 2).

The structure of the strand was further studied by TEM (Figure 3). The sharp selected-area electron diffraction (SAED) spots (Figure 3 a, upper inset) obtained from the center of the strand demonstrates that the solid Si core has a single-crystal structure, whereas the diffuse SAED pattern obtained from the edge of the strand (Figure 3 a, lower inset) reveals that the radially oriented SiO$_x$ nanowires standing on the core are an amorphous phase. According to statistical data from the TEM images, the Si core has an average diameter of 230 nm, and the SiO$_x$ nanowires in the shell have a uniform diameter of 10–20 nm and a length of hundreds of nanometers to several micrometers (with an aspect ratio of about 1000).

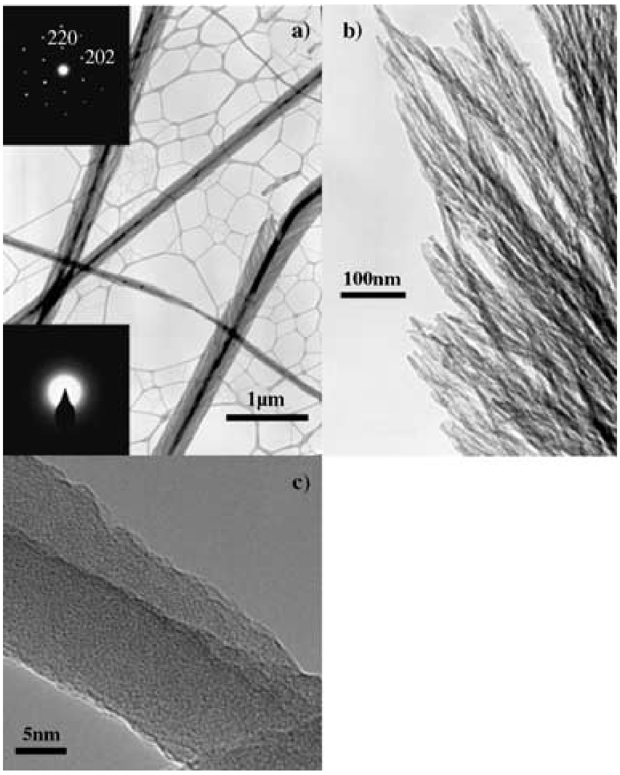

Figure 3. TEM images of the Si–SiO$_x$ hierarchical nanostructure. a) TEM image of the strands and corresponding selected-area electron diffraction pattern of the core (upper inset) and the shell (lower inset). b) TEM image of the aligned SiO$_x$ nanowires, detached from the shell of the cable by sonication. c) High-resolution TEM image of the amorphous SiO$_x$ nanowire showing its featureless structure.

An X-ray diffraction spectrum of the as-synthesized hierarchical structure is shown in Figure 4, which reveals that the sample is dominated by the cubic silicon phase. The spectrum also shows reflections due to the body-centered crystalline structure of Sn. These results are in good agreement with those of SAED and EDX.

To elucidate the growth mechanism of the hierarchical structure, the tip regions of the strands were examined in detail. Figure 5 shows a TEM image of a single strand

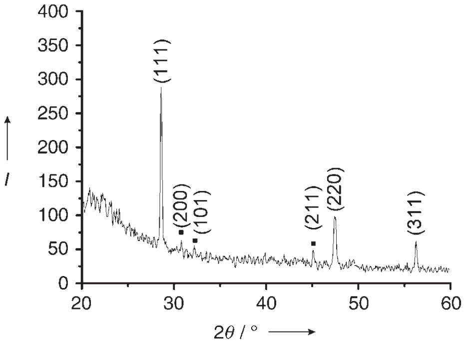

Figure 4. XRD spectrum of the Si–SiO$_x$ hierarchical nanostructure. The peaks marked by ■ belong to the body-centered crystalline structure of Sn, and the rest to crystalline Si. The weak, broad peak at 21° is due to amorphous SiO$_x$.

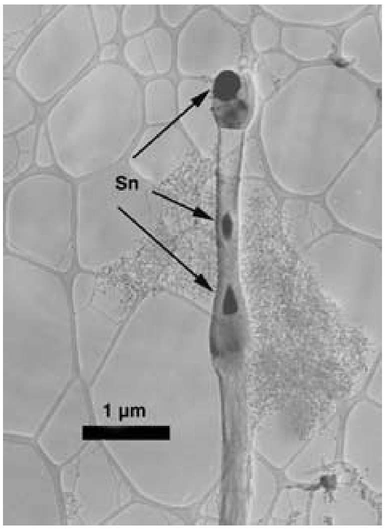

Figure 5. TEM image of the Si–SiO$_x$ hierarchical nanostructure or strand with a spherical Sn particle at the tip and Sn inside the strand.

segment, in which a spherical particle at the tip can be clearly observed. The chemical composition at several different positions was analyzed by EDX. The spherical particle at the tip of the strand is an Sn particle surrounded by Si. The Sn particle is considered to act as a catalyst for nanowire growth, because the corresponding eutectic Si–Sn alloy can form at low temperature (232 °C). The presence of a spherical metallic particle at the tip is usually considered to be a signature of the VLS mechanism.[5] The growth direction of the single-crystal Si core is (111), as determined by SAED, and is in good agreement with the VLS growth process.[5] The part of the nanotube partially filled with Sn between the spherical particle at the tip and the main product is due to the temperature change at the end of the preparation, as was previously observed.[5] Pan et al. also found that gallium catalyst could be wrapped inside Si in the synthesis of silicon oxide nanowire sandwich structures,[6] in which they attributed the growth of amorphous silicon oxide nanowires outside the Si core to oxidation of silicon. We suggest that the silicon oxide wires standing on the silicon core in the present case may also grow by the same oxidation process.

We now discuss why the SiO$_x$ nanostructure forms in a wirelike form instead of an agglomeration pattern. Previous models for explaining this phenomenon[6–11] suggested that Si reacts with oxygen to form SiO$_x$ particles, which then serve as nucleation sites to initiate the growth of SiO$_x$ nanowires. However, we suggest that the OAG process proposed by Lee et al.[12–14] may be more suitable to account for the formation of SiO$_x$ nanowires in the present work. In contrast to the conventional VLS mechanism, the OAG process relies on an oxide or a redox reaction instead of a catalytic metal or metal compound to assist the formation of nanowires. We propose that the Si nuclei formed at the Si droplet surface covered by the SiO$_2$ layer are similar to the nanoparticles, which then were oxidized to SiO$_x$ dots by reacting with the SiO$_2$ outside. Meanwhile, new Si extruded from the alloy would nucleate at the end of the nanoparticles. This recurrence or cycling process would maintain the continual growth of the amorphous SiO$_x$ nanowire. Meanwhile, the Si core would continue its growth along the axial direction, guided by the Sn catalyst and following the VLS mechanism, and only the surface nuclei could be formed when the core remained in the liquid state. Concurrent with core growth, the end of the SiO$_x$ nanowires grown from the surface nuclei would grow in the forward direction together. Consequently, the SiO$_x$ nanowires would form at an angle with respect to the growth direction of the core, just as was discussed above. According to the above analysis, we propose the following process for the formation of the Si–SiO$_x$ hierarchical structure, as shown schematically in Figure 6:

1) Thermal evaporation: vaporization of Sn and SiO powder to form Sn and SiO vapors.
2) Vapor deposition: deposition and formation of SiO-containing Sn liquid droplets in the low-temperature area (Figure 6 a).
3) Separation: disproportionation of SiO into SiO$_2$ + Si and subsequent phase separation of Si and SiO$_2$, whereby SiO$_2$ wraps the alloy droplet (Si and Sn; Figure 6 b).
4) Growth: precipitation and segregation of Si crystal from liquid Sn due to supersaturation of Si in the Sn + Si droplet (Figure 6 c). Then the SiO$_2$ species on the surface react with Si nuclei or residual oxygen to form SiO$_x$ nanowires. At the same time the central Si core would continue to grow by the VLS mechanism. The two concurrent processes would make the product grow in axial and lateral directions, and finally form an Si–SiO$_x$ hierarchical structure (Figure 6 d).

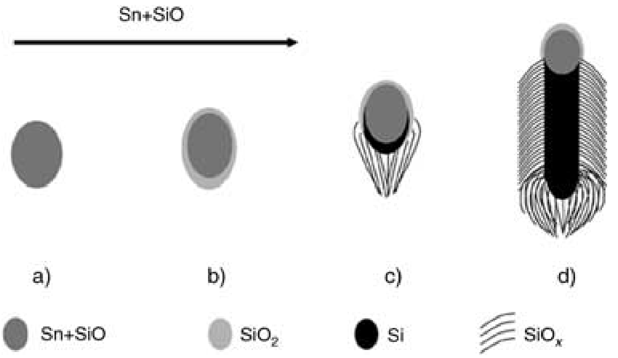

Figure 6. Proposed growth model for the Si–SiO$_x$ hierarchical structure. a) Sn and SiO vapors from the evaporation area (1320 °C) condense and form a liquid alloy droplet in the growing area (750–850 °C). b) More SiO vapor is absorbed into the droplet and disproportionates into Si and SiO$_2$, which are then phase-separated (at 800 °C, the concentration of Si in the Si/Sn alloy is about 1 %). c) Si nucleates and oxide grows into a SiO$_x$ nanowire. d) Single-crystal Si core grows with assistance of the Sn catalyst, and SiO$_x$ nanowires grow concurrently.

Figure 7 shows the room-temperature photoluminescence (PL) spectrum of the as-synthesized Si–SiO$_x$ hierarchical structures on excitation by a femtosecond laser at 300 nm. The spectrum is dominated by only one narrow UV emission peak centered at 378 nm with a half-peak width of 6 nm. This PL spectrum is radically different from that of nonhierarchical amorphous SiO$_2$ nanostructures, which usually show

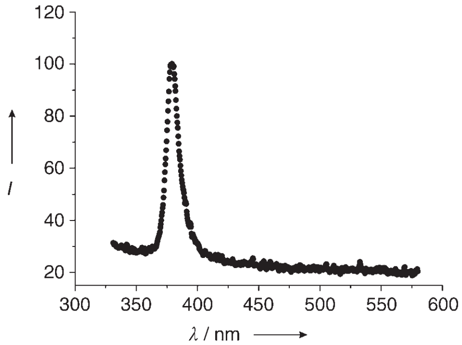

Figure 7. Photoluminescence spectrum of the Si–SiO$_x$ hierarchical nanostructure ($\lambda_{ex}=300$ nm).

multipeak blue or green emissions.[6,15] The nature of the UV PL peak is not clear, although several luminescence bands with peak energies ranging from 743 to 328 nm have been observed in various types of silica by Nishikawa et al.[16] On the other hand, the present emission centered at 378 nm may also be attributable to oxygen vacancies.[16]

In conclusion, a novel hierarchical nanostructure consisting of high-density amorphous silica nanowires radially standing on a single-crystal silicon core were grown on a substrate in bulk (grams) quantity by a simple thermal evaporation process. The nanostructure shows a single sharp PL peak at 378 nm. The microsized hierarchically ordered nanostructures of Si and its luminescent oxide could serve as potential building blocks for ready assembly into various functional devices. Indeed, the Si–SiO$_x$ hierarchical nanostructure has been shown to be an outstanding template for chemical and biosensors[18] due to its large surface-to-volume ratio. The present facile growth process is expected to be readily extendable to fabricate similar functional hierarchical nanostructures of other semiconductors and oxides.

Experimental Section

The Si–SiO$_x$ strands were synthesized in a high-temperature tube furnace, as described previously.[9] An Al_2O_3 boat with a mixture of 3.00 g SiO (Aldrich, 325 mesh, 99.9%) and 0.50 g Sn was put in the center of an alumina tube and then mounted in the furnace. The system was pumped to 5×10^{-2} mbar and than heated to 1320 °C at 40 °C min^{-1}, then a mixture of argon (95%) and hydrogen (5%) at 350 mbar was kept flowing at a rate of 10 sccm. After growth for about 7 h, the furnace was cooled to room temperature at 40 °C min^{-1}. A dark yellow product (ca. 0.5 g) was obtained on the silicon wafer and the inside wall of the alumina tube in the 750–850 °C zone at the downstream end; the amount of product can be increased by lengthening the reaction time. The product was checked by SEM (Philips XL 30 FEG) and XRD (Siemens D500). Some of the sample was dispersed in ethanol and a drop of the dispersion was put on a carbon-coated copper TEM sample grid for examination by TEM (Philips, CM20, operated at 200 kV). To record the room-temperature photoluminescence spectrum, the sample was fixed between two crystal plates, and a 3941C-M1BB/Spitfire FF-1K/OPA-800CF-0.5 femtosecond laser (300 nm) was used as excitation source.

Received: June 7, 2005
Revised: August 5, 2005

Keywords: crystal growth · luminescence · materials science · nanostructures · silicon

---

[1] a) A. M. Fennimore, T. D. Yuzvinsky, W.-Q. Han, M. S. Fuhrer, J. Cumings, A. Zettl, *Nature* **2003**, *424*, 408; b) Z. Zhong, D. Wang, Y. Cui, M. W. Bockrath, C. M. Lieber, *Science* **2003**, *302*, 1377; c) D. D. D. Ma, C. S. Lee, F. C. K. Au, S. Y. Tong, S. T. Lee, *Science* **2003**, *299*, 1874.
[2] a) P. Yang, *Nature* **2003**, *425*, 243; b) D. Whang, S. Jin, Y. Wu, C. M. Lieber, *Nano Lett.* **2003**, *3*, 1255; c) A. Tao, F. Kim, C. Hess, J. Goldberger, R. He, Y. Sun, Y. Xia, P. Yang, *Nano Lett.* **2003**, *3* 1229; d) Y. C. Zhu, Y. Bando, D. Feng Xue, D. Golberg, *Adv. Mater.* **2004**, *16*, 831.
[3] a) J. Q. Hu, Q. Li, X. M. Meng, C. S. Lee, S. T. Lee, *Chem. Mater.* **2003**, *15*, 305; b) J. Y. Lao, J. G. Wen, Z. F. Ren, *Nano Lett.* **2002**, *2*, 1287; c) Z. L. Wang, Z. W. Pan, *Adv. Mater.* **2002**, *14*, 1029; d) Y. Q. Zhu, W. K. Hsu, W. Z. Zhou, M. Terrones, H. W. Kroto, D. R. M. Walton, *Chem. Phys. Lett.* **2001**, *347*, 337; e) M. H. Huang, S. Mao, H. Feick, H. Yan, Y. Wu, H. Kind, E. Weber, R. Russo, P. Yang, *Science* **2001**, *292*, 1897; f) X. M. Meng, J. Q. Hu, Y. Jiang, C. S. Lee, S. T. Lee, *Appl. Phys. Lett.* **2003**, *83*, 2241; g) K. C. Kam, F. L. Deepak, A. K. Cheetham, C. N. R. Rao, *Chem. Phys. Lett.* **2004**, *397*, 329.
[4] C. Ye, L. Zhang, X. Fang, Y. Wang, P. Yan, J. Zhao, *Adv. Mater.* **2004**, *16*, 1019.
[5] a) Y. F. Zhang, Y. H. Tang, N. Wang, D. P. Yu, C. S. Lee, I. Bello, S. T. Lee, *Appl. Phys. Lett.* **1998**, *72*, 1835; b) R. S. Wagner, W. C. Ellis, *Appl. Phys. Lett.* **1964**, *4*, 89; c) Z. W. Pan, Z. R. Dai, C. Ma, Z. L. Wang, *J. Am. Chem. Soc.* **2002**, *124*, 1817.
[6] Z. W. Pan, S. Dai, D. B. Beach, D. H. Lowndes, *Appl. Phys. Lett.* **2003**, *83*, 3159.
[7] Z. W. Pan, S. Dai, D. B. Beach, D. H. Lowndes, *Nano Lett.* **2003**, *3*, 1279.
[8] B. Zheng, Y. Wu, P. Yang, J. Liu, *Adv. Mater.* **2002**, *14*, 122.
[9] X. H. Sun, C. P. Li, W. K. Wong, N. B. Wong, C. S. Lee, S. T. Lee, B. K. Teo, *J. Am. Chem. Soc.* **2002**, *124*, 14464.
[10] J. Q. Hu, X. M. Meng, Y. Jiang, C. S. Lee, S. T. Lee, *Adv. Mater.* **2003**, *15*, 70.
[11] C. Wu, W. Qin, G. Qin, D. Zhao, J. Zhang, W. Xu, H. Lin, *Chem. Phys. Lett.* **2003**, *378*, 368.
[12] S. T. Lee, Y. F. Zhang, N. Wang, Y. H. Tang, I. Bello, C. S. Lee, *J. Mater. Res.* **1999**, *14*, 4503.
[13] N. Wang, Y. H. Tang, Y. F. Zhang, C. S. Lee, S. T. Lee, *Phys. Rev. B* **1998**, *58*, R16024.
[14] R. Q. Zhang, Y. Lifshitz, S. T. Lee, *Adv. Mater.* **2003**, *15*, 635.
[15] a) J. Q. Hu, Y. Jiang, X. M. Meng, C. S. Lee, S. T. Lee, *Chem. Phys. Lett.* **2003**, *367*, 339; b) D. P. Yu, Q. L. Hang, Y. Ding, H. Z. Zhang, Z. G. Bai, J. J. Wang, Y. H. Zou, W. Qian, G. C. Xiong, S. Q. Feng, *Appl. Phys. Lett.* **1998**, *73*, 3076; c) J. Jang, H. Yoon, *Adv. Mater.* **2004**, *16*, 799.
[16] H. Nishikawa, T. Shiroyama, R. Nakamura, Y. Ohki, *Phys. Rev. B* **1992**, *45*, 586.
[17] a) S. Y. Ma, *Surf. Interface Anal.* **2001**, 31, 890; b) J. H. Stathis, M. A. Kastner, *Phys. Rev. B* **1987**, *35*, 2972.
[18] M. W. Shao et al., unpublished results.